Journal Website: https://www.icjn.net/bst ISSN: 3106-5112 | EISSN: 3106-5120

Biofeed Science and Technology (BST)

ICJN Press Volume. 01 | Issue. 02 | Aug. 2026 DOI: 10.66729/bst202606001

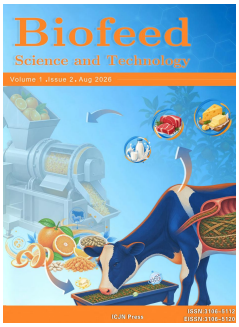

ARTICLE

Characterization of a Novel *CotA*-Type Laccase from the Safe *Bacillus velezensis* T-3 Via Genome Analysis, Quantitative Proteomics and Molecular Docking

Jiali Su[1,†], Yanhong Cao[2,†], Ngo Dinh Tan[3], Miao Liang[1], Qianyi Chen[1], Shasha Luo[1], Fengdie Huang[1], Xuewen Chen[1,4], Dong Luo[1], Caixia Zou[1], Xinghua Cai[1,*]

1 College of Animal Science and Technology, Guangxi University, Nanning Guangxi 530004, China.
2 Guangxi Agricultural Vocational University, Nanning Guangxi 530004, China.
3 Bavi Cattle and Forage Research Center, Hanoi 12632, Vietnam.
4 Guangxi UBIT Biotechnology Co., Ltd., Nanning Guangxi 530000, China.
† These authors contributed equally to this work.

*Corresponding Author: Xinghua Cai, E-mail: 13367811557@163.com

Abstract

Laccase is a class of known copper-dependent oxidase which can antagonize molds and degrade mycotoxins efficiently, but few reports exist on the structure and function of laccase from *Bacillus velezensis*. In this study, we identified a *CotA*-type laccase gene (locus tag: *ctg*_03438) in *B. velezensis* T-3, and its DON removal capacity was investigated via bioinformatics analysis, 4D-DIA quantitative proteomics, and in vitro fermentation assays. Results indicated that the *CotA* gene encodes an extracellular spore coat protein (*CotA*) that lacks typical signal peptides and transmembrane domains. Crucially, 4D-DIA quantitative proteomic analysis confirmed that *CotA* in *B. velezensis* T-3 is expressed at a high level, with 23 unique peptides covering 47.30% of the protein sequence, including a strictly proteotypic peptide (PLKEADTSRK). Molecular docking revealed a stable DON-*CotA* interaction (ΔG = -6.299 kcal/mol) with a 6.4 Å distance to the T1 copper center, suggesting a potential binding mode for DON recognition. Functionally, *B. velezensis* T-3 demonstrated potent antifungal activity (inhibition zone: 3.51 cm against *Fusarium graminearum* (*F. graminearum*)) and achieved a 30.06% reduction of DON in contaminated feed within 10 days. This study provides a safe candidate strain and molecular-level evidence for the development of biodetoxification agents.

Keywords

Bacillus velezensis; Laccase; *CotA*; Deoxynivalenol

Citation: Jiali Su, Yanhong Cao, Ngo Dinh Tan, *et al*. Characterization of a Novel *CotA*-Type Laccase from the Safe *Bacillus velezensis* T-3 Via Genome Analysis, Quantitative Proteomics and Molecular Docking. *Biofeed Science and Technology*. 2026, 01 (2): 1-12. doi: 10.66729/bst202606001.

Copyright:© 2026 The Author(s). Published by ICJN Press.
This is an open access article under the https://creativecommons.org/licenses/by/4.0/
Received 28 May 2026; Revised 15 June 2026; Accepted 16 July 2026; Available online 31 August 2026.

Graphical Abstract

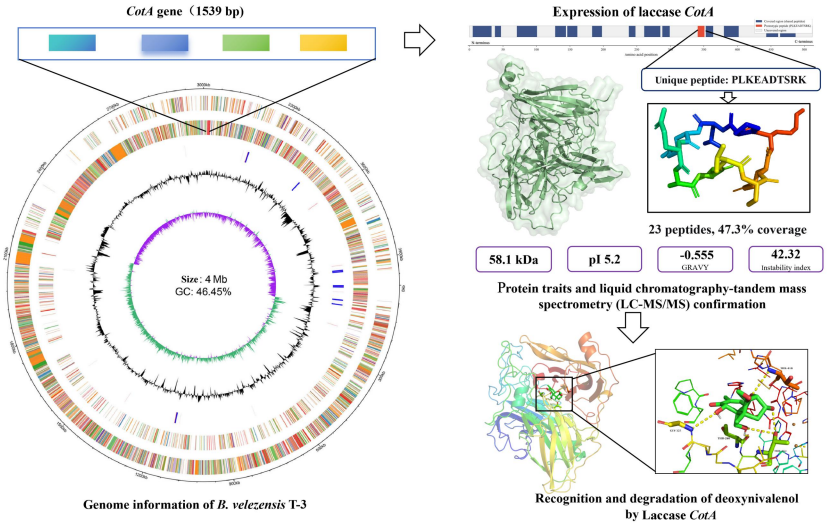

Highlights

- A novel *CotA*-type laccase gene was identified in *B. velezensis* T-3.
- 4D-DIA proteomics confirmed *CotA* translation with 47.30% coverage.
- Docking showed stable DON binding to T1 Cu (6.4 Å, ΔG = -6.3 kcal/mol).
- T-3 inhibited three toxigenic fungi and degraded 30.06% DON in feed.

1. Introduction

Deoxynivalenol (DON) is one of the most prevalent trichothecene mycotoxins produced by *Fusarium* species and is frequently detected in cereals, animal feed, and processed food commodities. Its global persistence stems from high natural occurrence, exceptional chemical stability, and resistance to conventional thermal and mechanical processing techniques[1]. Accumulating toxicological evidence now associates chronic DON exposure with adverse effects including intestinal barrier dysfunction, immunomodulatory disturbances, hepatotoxicity, and neurobehavioral alterations, thereby compromising livestock productivity, feed safety, and the integrity of the human food supply chain. Although physical (e.g., sorting, milling) and chemical (e.g., ozonation, alkaline treatment) detoxification strategies can achieve partial DON reduction, their practical implementation is limited by poor specificity, concomitant degradation of essential nutrients, incomplete toxin removal, or generation of toxic transformation products. In contrast, biological detoxification, particularly enzymatic biotransformation, has emerged as a promising alternative, enabling selective, efficient, and environmentally benign degradation of DON under mild operational conditions[2]. However, the discovery and characterization of microbial enzymes exhibiting high catalytic efficiency, substrate specificity, and stability toward DON remain challenging; thus, identifying and engineering robust DON-transforming enzymes continues to be a critical research priority for advancing sustainable mitigation strategies in agricultural production and feed manufacturing systems.

To date, microbial enzymes implicated in DON detoxification have been classified into several functionally distinct categories, each targeting specific functional groups or structural motifs within the mycotoxin molecule[3]. A well-characterized example is the fungal glutathione S-transferase Fhb7. Yang *et al*. resolved its crystal structure at 2.41 Å resolution and, through site-directed mutagenesis, established that Arg68 is essential for catalytic activity; substitution of this residue completely abrogates enzymatic function, providing direct structural and functional evidence that Fhb7 selectively targets the C12-C13 epoxide moiety of DON[4]. Furthermore, enzyme stability was identified as a critical determinant of biotechnological applicability: engineered variants V29P and M10 exhibited half-lives approximately 5.5-fold and 266.7-fold longer than that of wild-type Fhb7, respectively. Functional validation in recombinant expression systems revealed that *Bacillus subtilis* WB600 expressing M10 degraded ~72% of DON within 72 h, whereas *Escherichia coli* harboring the same construct achieved complete (i.e., undetectable) DON removal under identical conditions. Beyond Fhb7-like glutathione transferases, bacterial *DepA/DepB* enzymatic pathways mediate sequential DON transformation, first to 3-keto-DON and subsequently to 3-epi-DON. Plant-derived glyoxalase-like enzymes further demonstrate that DON detoxification can proceed via diverse biochemical routes, including oxidation, reduction, and stereochemical inversion, indicating the absence of a single conserved mechanism. Among oxidative biocatalysts, laccases are especially promising owing to their broad substrate tolerance and proven suitability for rational engineering. For instance, the bacterial laccase Lac-W from *Weizmannia coagulans* directly degraded 34% of DON within 24 h in the absence of redox mediators. Subsequent studies showed that, in the presence of ABTS alone, Lac-W achieved 51% degradation; with a dual-mediator system (AS + ABTS), degradation increased to 68%; and in a maize-based matrix, DON removal reached ~66%[5,6]. Similarly, Shanakhat *et al*. demonstrated that a fungal laccase

coupled with TEMPO effectively modified DON, reinforcing the cross-kingdom feasibility of laccase-mediated DON transformation[7]. Nevertheless, currently characterized laccases with experimentally confirmed activity against mycotoxins remain largely restricted to fungal species and a narrow subset of bacteria. Their catalytic efficiencies vary substantially depending on enzyme origin, mediator dependency, and complexity of the reaction matrix. Notably, within the genus *Bacillus*, recent advances in mycotoxin biodegradation have been more pronounced for zearalenone than for DON. For example, Wei *et al*., identified two zearalenone-degrading enzymes from *Bacillus velezensis* B.26, including a *CotA*-like laccase that removed 91.94% of 5 μg/mL zearalenone within 6 h at 70 ℃ and pH 8.0; LC-MS analysis confirmed the formation of low-toxicity derivatives and the absence of hazardous byproducts such as α-zearalenol (α-ZEL) or α-zearalanol (α-ZAL)[8]. Collectively, these findings indicate that known microbial DON-detoxifying enzymes fall primarily into four functional classes: (i) Fhb7-like glutathione S-transferases, (ii) *DepA/DepB*-type oxidoreductases, (iii) glyoxalase-related isomerases/rearrangement enzymes, and (iv) laccase-catalyzed oxidative systems. However, reports on laccases from *B. velezensis*, particularly regarding their three-dimensional architecture, substrate-binding determinants, and molecular basis for DON recognition and turnover, remain notably scarce.

This knowledge gap is particularly salient in the context of probiotic *Bacillus* resources isolated from marine animal gastrointestinal tracts. Cai *et al*. recently reported that *B. velezensis* strain T-3, originating from the gut microbiota of the sea cucumber *Apostichopus japonicus*, exhibits potent antagonistic activity against the mycotoxigenic fungi *Fusarium graminearum* (*F. graminearum*) and *Penicillium chrysogenum*[9]. Quantitative LC-MS/MS analysis demonstrated that DON was completely eliminated within 72 h of incubation, as evidenced by the reduction of the DON peak area from 8,348,311 at time zero to undetectable levels, indicating near-total biotransformation rather than mere adsorption. Furthermore, metabolomic profiling revealed 36 significantly upregulated metabolites under DON, as sole carbon-source conditions, while functional annotation identified 108 carbohydrate-active enzymes, collectively supporting a model wherein DON degradation is tightly coupled with broad-scale metabolic reprogramming. In our prior study, the same safe, non-pathogenic *B. velezensis* T-3 strain was characterized for dual functionality: antifungal activity against toxigenic molds and efficient DON removal in liquid fermentation systems. Whole-genome sequencing uncovered a previously unannotated *CotA* gene encoding a putative *CotA*-type multicopper laccase. Building on these findings, the present study employs an integrated approach, including comparative genomic annotation, evolutionary sequence conservation analysis, homology-based structural modeling, ligand-enzyme molecular docking simulations, and targeted fermentation assays, to decipher the structural determinants underlying DON recognition and catalytic transformation by the *CotA* laccase. Elucidating this structure-function relationship not only expands the sparse catalog of functionally validated *B. velezensis* laccases involved in trichothecene detoxification but also establishes a foundation for rational enzyme engineering and the development of feed-oriented biodetoxification strategies. The novelty of this study lies in the integrative evidence of proteomic validation, functional phenotype, and structural prediction for this specific *CotA* homolog, rather than in primary sequence alone.

2. Materials and Methods

2.1 Strains and Culture Conditions

B. velezensis T-3 was isolated from sea cucumber gut and was deposited in the Guangdong Microbial Culture Collection Center (GDMCC No. 62955). The safety profile of this strain, including hemolytic activity, antibiotic susceptibility, and genome-wide virulence factor screening, has been previously characterized and reported[9]. For activation, the strain was cultured in LB liquid medium (37 ℃, 180 rpm). Indicator fungi, including *F. graminearum*, *Aspergillus flavus* (*A. flavus*), and *Penicillium viridicatum* (*P. viridicatum*), were purchased from the China Center for Industrial Culture Collection (CICC). The indicator fungi were cultured on potato dextrose agar (PDA) medium at 28 ℃ for 5−7 days for subsequent use.

2.2 Genome Annotation of *B. velezensis* T-3

Genome annotation of *B. velezensis* T-3 was completed prior to this study. Annotation results integrated data from the Non-Redundant protein sequence database (NR), Swiss-Prot, Clusters of Orthologous Groups (COG), Gene Ontology (GO), Kyoto Encyclopedia of Genes and Genomes (KEGG), and Pfam databases, obtained the following information: whole genome sequence, gene coordinate annotation file, protein sequences of all predicted genes, based on the above information, the gene function information of *B. velezensis* T-3 has been compiled.

2.3 Laccase Gene Screening and Sequence Analysis

Candidate laccase genes were screened from the functional annotation table using keywords including "laccase" "multicopper oxidase" and "*CotA*". Candidate genes were further validated by BLASTP against the National Center for Biotechnology Information (NCBI) nr database (https://www.ncbi.nlm.nih.gov/). The *CotA* gene (locus tag: *ctg_03438*) was selected for further analysis. Signal peptides, transmembrane domains, and subcellular localization were predicted using SignalP 6.0[10], DeepTMHMM, and DeepLoc-Pro 1.0, respectively[2,11]. Domain annotation was performed with InterProScan, and physicochemical properties were analyzed with ProtParam[12,13].

2.4 Proteomic Validation of *CotA* Expression

B. velezensis T-3 samples preserved at -80 ℃ were ground into fine powder in liquid nitrogen. The cell powder was transferred into 1.5 mL tubes and lysed with SDT buffer (4% SDS, 100 mM Tris-HCl, 10 mM DTT, 1 mM PMSF, and 2 mM EDTA). After vortexing, the mixture was boiled at 95 ℃ for 15 min, followed by ultrasonication on ice for 10 min. The supernatant was collected by centrifugation as the total protein extract. Four volumes of cold acetone were added to the extract, and proteins were precipitated overnight at -20 ℃. After centrifugation at 4 ℃, the pellet was washed three times with cold acetone and then dissolved again in 8M urea. Total protein concentration was determined using a BCA kit (Beyotime Biotechnology, Shanghai, China).

For enzymatic digestion, 100 μg of protein solution was adjusted to 200 μL with 8 M urea. Dithiothreitol (DTT) was added to a final concentration of 5 mM, and the mixture was incubated at 37 ℃ for 45 min. Subsequently, iodoacetamide (IAM) was added to 11 mM, and alkylation was performed at room temperature in the dark for 15 min. The reaction was diluted with 800 μL of 25 mM ammonium bicarbonate, followed by addition of 2 μL trypsin (Promega Corporation, Madison, WI, USA) and overnight digestion

at 37 °C. The resulting peptides were acidified with 20% trifluoroacetic acid (TFA) to pH 2−3, desalted using C18 spin columns (Millipore, Billerica, MA, USA), and quantified with a Pierce™ Quantitative Peptide Assay kit (Thermo Fisher Scientific, USA).

LC-MS/MS analysis was performed on a NanoElute UHPLC system (Bruker Daltonics, Germany) coupled to a timsTOF Pro2 mass spectrometer (Bruker Daltonics, Germany). Mobile phase A was 0.10% formic acid in water, and mobile phase B was 0.10% formic acid in acetonitrile. Peptides (200 ng) were loaded onto an analytical column (IonOpticks, Australia, 15 cm × 75 μm, 1.6 μm C18) and separated at 50 °C with a flow rate of 500 nL/min using a 20 min gradient: 5%−25% B in 0−17 min, 25%−40% B in 17 min−18 min, 40%−95% B in 18−19 min, and 95% B held for 19−20 min. MS data were acquired in positive-ion mode with a mass range of 100−1,700 m/z and an ion mobility range of 0.85−1.30 Vs/cm^2. The capillary voltage was set to 1,500 V, drying gas flow to 3 L/min, and drying temperature to 180 °C. The data-independent acquisition parallel accumulation-serial fragmentation (diaPASEF) scheme comprised 48 acquisition windows, with collision energy linearly increasing from 27 eV (1/K0 = 0.85) to 45 eV (1/K0 = 1.30).

Raw MS data were analyzed using DIA-NN (v1.8.1)[14] in library-free mode against the *B. velezensis* UniProtKB proteome (Taxonomy ID: 492670, 18,047 sequences, downloaded Nov 19, 2025). Spectral library prediction based on deep learning and match-between-runs (MBR) was enabled. Precursor and protein false discovery rates (FDR) were controlled at < 1%. Protein quantification was performed using the MaxLFQ algorithm with normalization within each sample.

2.5 Phylogenetic Analysis

Homologous *CotA* sequences from the genus *Bacillus* were downloaded from the NCBI nr database. Multiple sequence alignment was performed using MEGA 7.0 with the MUSCLE algorithm. After alignment, both ends were manually trimmed to retain conserved regions. A Neighbor-Joining (NJ) phylogenetic tree was constructed with 1,000 bootstrap replicates, and gaps were treated by complete deletion. Bootstrap support values (≥ 50%) are indicated at the nodes[15].

2.6 Multiple Sequence Alignment

To further validate the conservation of the *CotA* protein from *B. velezensis* T-3, multiple sequence alignment was performed with three representative *CotA* laccase sequences: laccase from *B. velezensis* FZB42 (UniProt ID: A7Z229), the sequence in NCBI, which is an outer spore coat copper-dependent laccase *CotA* from *Bacillus* (GenBank ID: WP_060562950.1), and the classical *CotA* sequence from *Bacillus subtilis,* which has been well characterized. (UniProt ID: P07788). Multiple sequence alignment of these four sequences was conducted using ClustalW (https://www.ebi.ac.uk/Tools/msa/clustalo/) with default parameters[16]. The alignment results were visualized and annotated using ESPript 3.0 (https://espript.ibcp.fr), with particular attention to the conservation of copper-coordinating residues (histidine, cysteine) and substrate-binding residues predicted by molecular docking[17].

2.7 3D Structure Modeling and Molecular Docking Analysis

The 3D structure of the *CotA* protein in *B. velezensis* T-3 was predicted using the AlphaFold3 online server, yielding a model with high confidence and a pTM score of 0.97[18]. As the predicted model lacked copper ions, a BLAST search of the *CotA* protein sequence against the UniProt database revealed that the known structure with the highest similarity was the laccase from *B. velezensis* FZB42 (UniProt ID: A7Z229, 99% sequence similarity). Its crystal structure contains four complete copper ions. In PyMOL lvisualization analysis, the AlphaFold model was aligned with the A7Z229 crystal structure using Cα atoms (align command). Based on the alignment, four copper ions from the A7Z229 structure were precisely copied to corresponding positions in the predicted model using create command, generating an intermediate file containing copper co-factors. The receptor file including copper ions was then prepared by adding hydrogens and optimizing the hydrogen bond network at pH 4.5 using UCSF Chimera[19]. DON was prepared at pH 4.5.

The 3D structure of DON was obtained from the PubChem database (CID: 40024)[20] and converted to mol2 format using PyMOL[21]. Molecular docking analysis was performed on the SwissDock platform (https://www.swissdock.ch/), powered by the AutoDock Vina engine[22,23]. The docking box was centered at the T1 copper coordinates with dimensions of 20 Å × 20 Å × 20 Å. The conformation with the lowest binding free energy was selected as the optimal binding mode. Hydrogen bond interactions and the distance between substrate and T1 copper were analyzed in PyMOL.

2.8. Antifungal Test of *B. velezensis* T-3

Plate confrontation assays were used to determine the antagonistic activity of *B. velezensis* T-3 against three toxigenic fungi, including *F. graminearum*, *A. flavus*, and *P. viridicatum*. Specifically, the fungus was inoculated on different PDA plates, followed by the T-3 bacterial suspension (10 μL, OD_{600} = 1.0) were inoculated. After 5 days of incubation at 28 °C, the diameter of inhibition zone and the fungal colony diameter were measured to evaluate the antifungal activity of *B. velezensis* T-3. The diameters of inhibition zones and fungal colonies were measured by the cross-streaking method: two perpendicular diameters were recorded for each zone and colony, and the average value was used. For each fungal species, a control plate (fungus inoculated without bacterial suspension) was included to measure the normal colony diameter (d). The inhibition zone diameter (D) was measured from the test plates (fungus + bacteria). The D/d ratio was calculated as inhibition zone diameter / colony diameter. The inhibition rate was calculated as: Inhibition rate (%) = [(d_control − d_test) / d_control] × 100. All experiments were performed in three independent biological replicates.

2.9. Verification of the DON Removal Rate in Feed

Moldy molasses pomace feed with high DON content (3,000−5,000 μg/kg) was selected, which was dried and sterilized at high temperature as the main fermentation substrate. Subsequently, *F. graminearum suspension* was inoculated first, and then 0%, 5% and 10% *B. velezensis* T-3 suspension were inoculated respectively. Sterile water was added to replace the bacterial suspension in the control group. All samples were put at 30°C for static fermentation for 10 days. The number of live molds was detected by plate counting method, and the change of DON content was detected by enzyme-linked immunosorbent assay (ELISA) to evaluate the removal rate of DON by *B. velezensis* T-3.

3. Results

3.1 Laccase Gene Identification in *B. velezensis* T-3

Via searching the whole genome functional annotation table with the keyword “laccase”, two candidate genes were yielded including *ctg_02518* and *ctg_03438*. Results indicated that

ctg_03438 was consistently annotated as "outer spore coat copper-dependent laccase *CotA*", with KEGG orthology K06324 (*CotA*) and Pfam domains including PF07732, PF00394, and PF07731, which are three typical multicopper oxidase domains. BLASTP alignment showed that the encoded protein shares 99% sequence identity with the *CotA* laccase from *B. velezensis* FZB42 (A7Z229), confirming it is the target gene (**Table 1**). This gene was therefore designated as the *CotA* gene of *B. velezensis* T-3.

Table 1. Functional annotation of the *CotA* gene in *B. velezensis* T–3

Database	Entry	Description
KEGG	K06324	*CotA*, spore coat protein A, manganese oxidase
Pfam	PF00394, PF07732, PF07731	Multicopper oxidase domains
COG	COG2132	Multicopper oxidase (contains three cupredoxin domains)
NR	WP_060562950.1	Outer spore coat copper-dependent laccase *CotA*
Swiss-Prot	A0A222C745	Laccase

NOTE: KEGG: Kyoto Encyclopedia of Genes and Genomes; Pfam: the Pfam protein families database; COG: Clusters of Orthologous Groups; NR: Non-Redundant protein sequence database.

3.2 Sequence Characteristics and Subcellular Localization

SignalP 6.0 prediction results of the *CotA* protein indicated that it lacks a typical signal peptide (Other probability 1.0, **Figure. 1(A)**), ruling out Sec or Tat secretion pathways. DeepTMHMM analysis showed no transmembrane helices across the entire sequence, with all residues located on the outside of the cell (**Figure. 1(B)**). DeepLoc-Pro predicted it as an extracellular protein with a probability of 0.8459 (**Figure. 1(C)**). These results suggested that the protein might be localized to the cell surface or extracellular environment through a non-classical pathway (e.g., spore coat assembly), enabling direct contact with and degradation of environmental toxins.

As shown in the **Figure. 1(D)**, InterProScan analysis revealed that the *CotA* protein contains three typical multicopper oxidase domains: PF07732, PF00394, and PF07731. InterProScan prediction also indicated copper-binding sites (PS00079). GO terms included GO: 0005507 (copper ion binding) and GO: 0016491 (oxidoreductase activity), consistent with laccase characteristics. ProtParam analysis showed that the protein consists of 512 amino acids, with a molecular weight of approximately 56 kDa and a theoretical isoelectric point of approximately 5.2 (64 negatively charged residues, 56 positively charged residues). The grand average of hydropathicity (GRAVY) is -0.555, indicating a hydrophilic protein. The instability index is 42.32, slightly above the threshold, but the conformation may become stable after binding copper ions. The molar extinction coefficient ε = 84,020 $M^{-1}\cdot cm^{-1}$ (oxidized state) suggests the presence of a relatively high number of aromatic amino acids.

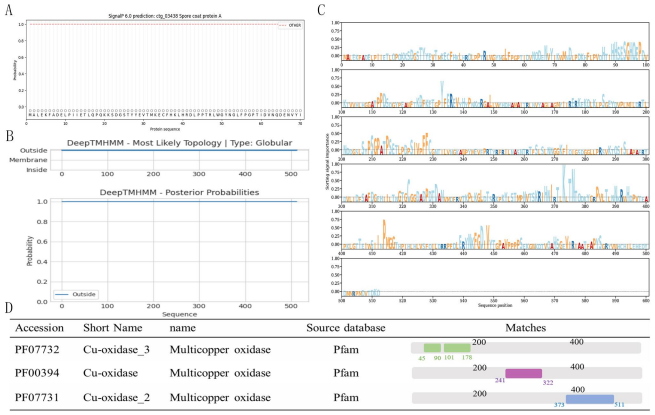

Figure. 1 Sequence features and domain architecture of *CotA* in *B. velezensis* T-3. (A) SignalP 6.0 prediction; (B) DeepTMHMM analysis; (C) DeepLoc-Pro 1.0 prediction; (D) InterProScan identification. **NOTE:** Pfam: the Pfam protein families database; TMHMM: Transmembrane Hidden Markov Model. Copyright: This figure was created by the authors based on the amino acid sequence of *CotA* from *B. velezensis* T-3 using the following online servers: Figure. 1(A) was generated using SignalP 6.0. (https://services.healthtech.dtu.dk/services/SignalP-6.0/); Figure. 1(B) using DeepTMHMM. (https://dtu.biolib.com/DeepTMHMM); Figure. 1(C) using DeepLoc-Pro 1.0. (https://services.healthtech.dtu.dk/services/DeepLocPro-1.0/); Figure. 1(D) using InterProScan 5. (https://www.ebi.ac.uk/interpro/).

3.3 Proteomic Validation of *CotA* Expression

To confirm whether the predicted *CotA* gene (locus tag: *ctg*_03438) is actively translated under routine culture conditions, we performed 4D- DIA quantitative proteomic analysis on whole-cell lysates of *B. velezensis* T-3. The laccase *CotA* protein (UniProtKB entry: A0ABC8D2A3, gene name: BVDSYZ_03405) was unequivocally identified. Sequence alignment demonstrated that the protein identified by proteomics shares 100% coverage and 99.22% sequence identity with the *CotA* gene product (E- value = 0.0), confirming that they represent the same protein.

A total of 23 unique and shared peptides mapping to *CotA* were detected with high confidence (after we removed duplicate entries and accounted for pot-translational modifications), covering 242 out of 512 amino acid residues (sequence coverage of 47.30%), with peptides distributed evenly from the N-terminus to the C-terminus (**Figure. 2(A), 2(B)**).

Among these, a strictly proteotypic peptide, PLKEADTSRK (residues 342-351), was uniquely matched to A0ABC8D2A3 with an intensity of 10,869.30, providing definitive evidence for authentic expression of *CotA* in *B. velezensis* T-3. Peptide intensity analysis further revealed high abundance of peptides derived from *CotA* (**Figure. 2(C)**), with the most intense peptide being FADELPIIETLQPQK (intensity = 84,488.9), followed by AWPYMEVEPR (44,920.5). The cumulative intensity of all 23 peptides reached 376,929, indicating a considerable expression level of *CotA* in *B. velezensis* T-3. Collectively, these proteomic data provide evidence that the *CotA* gene is actively translated into the *CotA* protein in *B. velezensis* T-3 under standard culture conditions.

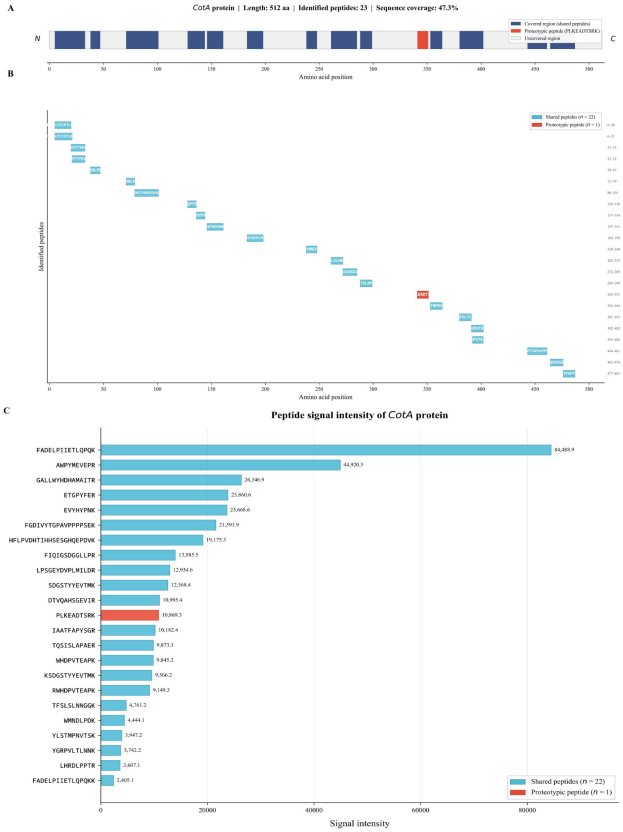

Figure. 2 Peptide coverage map of the *CotA* protein identified by 4D-DIA quantitative proteomics. (A) Schematic representation of the *CotA* protein sequence coverage; (B) Detailed mapping of the 23 identified peptides along the *CotA* amino acid sequence; (C) Signal intensity distribution of the identified peptides for the *CotA* protein. Blue bars represent shared peptides (n = 22). The orange bar represents the proteotypic peptide (PLKEADTSRK). **Note:** N: N-terminus; C: C-terminus. Copyright: This figure was created by the authors based on 4D-DIA quantitative proteomic data, with data visualization and layout performed using GraphPad Prism 8.0.

3.4. Phylogenetic Analysis

To determine the phylogenetic position of the *CotA* gene (*ctg*_03438) from *B. velezensis* T-3, a Neighbor-Joining (NJ) phylogenetic tree was constructed based on the amino acid sequences of the encoded protein and representative homologous sequences from *Bacillus* and related genera (**Figure. 3**). The results showed that *CotA* (T-3) clustered tightly with two previously reported spore coat proteins from *B. velezensis* (ASB64164.1 and ASB52011.1), forming a distinct clade with 100% bootstrap support, indicating a high degree of conservation within *B. velezensis* species. At the next hierarchical level, the clade containing *CotA* (T-3) (81% bootstrap support) included *CotA* homologs from *Bacillus nakamurai*, *Bacillus atrophaeus*, and *Bacillus halotolerans*. Additional branches, supported by bootstrap values of 63, 96, and 51, respectively, comprised multicopper oxidase family proteins from other *Bacillus* species and closely related genera such as *Oceanobacillus*, *Virgibacillus*, and *Halobacillus*. Collectively, these results unequivocally assign the *CotA* (T-3)-encoded protein to the *B. velezensis*-specific *CotA*-type laccase clade, fully consistent with its functional annotation.

Figure. 3 Neighbor-Joining phylogenetic tree based on *CotA* amino acid sequences. Copyright: This figure was created by the authors based on homologous *CotA* amino acid sequences, constructed using the Neighbor-Joining method in MEGA 7.0 with 1,000 bootstrap replicates, and the tree was refined and exported using the iTOL online platform. (https://itol.embl.de/).

3.5 Conservation Analysis of the Key Catalytic Residues of laccase *CotA*

To validate the functional conservation of laccase *CotA* in *B. velezensis* T-3, it was subjected to multiple sequence alignment with three representative laccases (A7Z229, WP_060562950.1, P07788) and visualized using ESPript 3.0 (**Figure. 4**). The alignment results showed that all histidine and cysteine residues involved in copper ion coordination (including His419, Cys492, His497 of the T1 copper center, and His86, His88, His140 of the trinuclear copper cluster) were completely conserved across the four proteins. Notably, the DON-binding residues predicted by molecular docking (THR260, THR262, GLY323, and THR418, numbered according to the *CotA* sequence in *B. velezensis* T-3) were also highly conserved in all aligned sequences. These results indicated that it possesses a complete copper ion binding network and highly conserved substrate recognition sites, further supporting its identity as a *CotA* protein with potential for DON degradation.

Figure. 4 Multiple sequence alignment of the *CotA* laccase from *B. velezensis* T-3 with three representative laccases (A7Z229, WP_060562950.1, P07788) using ClustalW and ESPript 3.0. **Note**: Yellow asterisks indicate completely conserved copper-coordinating residues (T1 center: His419, Cys492, His497; trinuclear cluster: His86, His140). Blue asterisks indicate highly conserved DON-binding residues predicted by molecular docking (THR260, THR262, GLY323, THR418). Copyright: This figure was created by the authors based on multiple sequence alignment results generated by ClustalW, rendered using ESPript 3.0. (https://espript.ibcp.fr).

3.6 3D Structure and Molecular Docking of the Laccase *CotA*

As shown in **Figure. 4**, the AlphaFold3-predicted model of the *CotA* (pTM = 0.97) exhibited a typical laccase globular fold, composed of three cupredoxin domains. After homologous alignment and introduction of four copper ions, a receptor model with a complete copper center was obtained (**Figure. 5A**). Molecular docking results (**Figure. 5(B)**, **5(C)**) showed that the optimal binding conformation of DON with the *CotA* had a binding energy of -6.299 kcal/mol, corresponding to a dissociation constant Kd ≈ 24.2 μM, indicating moderate binding strength. Moreover, DON formed hydrogen bonds with multiple polar residues in the active pocket (GLY323, THR260, THR418, THR262) (**Table 2**). The shortest hydrogen bond (THR260, 2.2 Å) may be crucial for substrate recognition. The closest atomic distance between the DON molecule and the T1 copper was 6.4 Å, which falls within the range where laccase electron transfer can occur (4 Å - 8 Å)[4], suggesting that this binding mode possesses catalytic potential. Suggesting that this binding mode is compatible with substrate accommodation and potential electron transfer.

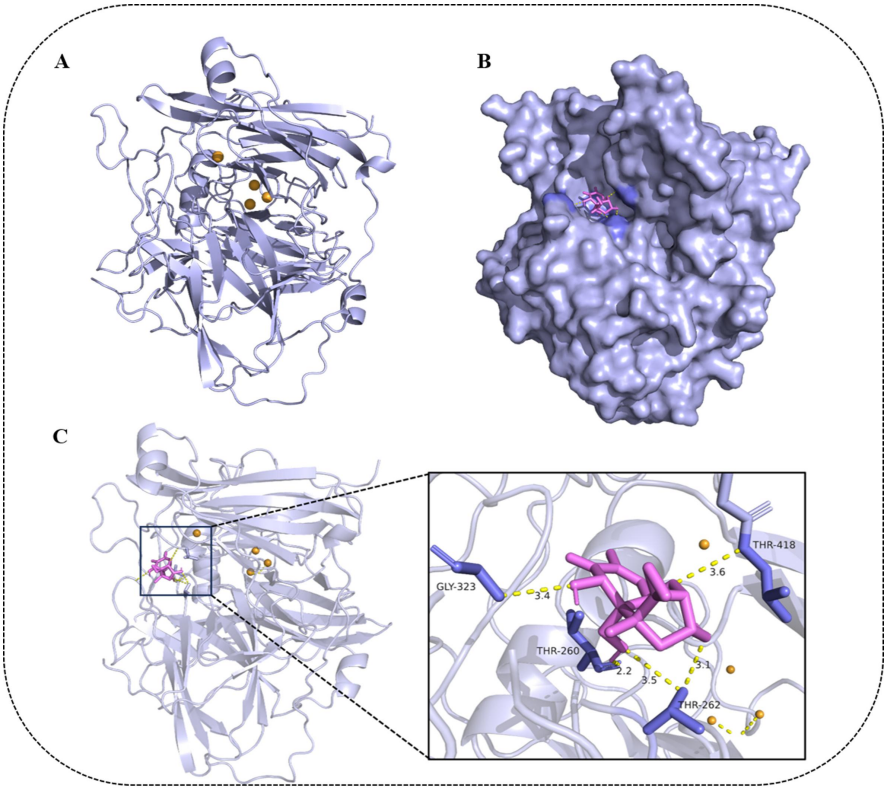

Figure. 5 Structural basis for DON binding to the laccase *CotA* in *B. velezensis* T-3; (A) Cartoon representation of the AlphaFold3-predicted structure of *CotA* with four copper ions; (B) Surface representation of the active site pocket with DON; (C) Hydrogen bonding network between DON and active-site residues. **NOTE:** Hydrogen bonds are shown as yellow dashed lines with distances (Å); DON: Deoxynivalenol. Copyright: This figure was created by the authors based on the amino acid sequence of *CotA* from *B. velezensis* T-3. The three-dimensional structure was predicted using the AlphaFold3 online server. Visualization and docking analysis were performed using PyMOL. Copper ion coordinates were referenced from the crystal structure of the characterized laccase from *B. velezensis* FZB42 (UniProt ID: A7Z229).

Table 2. Hydrogen bonds formed between DON and laccase *CotA* in molecular docking

Donor	Acceptor	Distance (Å)
DON (OH)	GLY323	3.40
DON (OH)	THR260	2.20
DON (OH)	THR418	3.60
DON (OH)	THR262	3.50
DON (OH)	THR262	3.10

NOTE: OH: Hydroxyl group.

3.7. Antifungal Activity and DON Removal Capacity of *B. velezensis* T-3

The antagonistic effects of *B. velezensis* T-3 against three representative toxigenic fungi were evaluated using plate confrontation assays (**Figure. 6(A)−(C)**). *B. velezensis* T-3 exhibited potent inhibitory activity against *P. viridicatum*, *F. graminearum*, and *A. flavus*, with clear inhibition zones surrounding the bacterial inoculum. The ratios of inhibition zone diameter to colony diameter (D/d) were determined to be 2.36, 2.50, and 2.97, respectively, with the strongest inhibition observed against *A. flavus* (D/d = 2.97). The corresponding inhibition rates were 58.50% (*P. viridicatum*), 60% (*F. graminearum*), and 66.30% (*A. flavus*), respectively. These results indicate that T-3 possesses broad-spectrum antifungal activity against filamentous mycotoxigenic fungi.

The ability of *B. velezensis* T-3 to degrade DON was assessed in a moldy feed fermentation system with an initial DON concentration ranging from 3,700 to 3,900 μg/kg (**Figure 6(D)**). In the control group (0% inoculum), DON levels remained relatively stable throughout the 10-day fermentation period. Inoculation with 5% T-3 suspension resulted in DON removal rates of 8.37% and 21.50% after 5 and 10 days, respectively. When the inoculum size was increased to 10%, the removal rates reached 8.11% (5 days) and 30.06% (10 days). Collectively, these findings demonstrate that *B. velezensis* T-3 not only suppresses the growth of toxigenic fungi but also effectively degrades DON in a feed matrix, with detoxification efficiency showing clear patterns that depend on inoculum and time.

Tested fungus	Inhibition zone diameter (cm, D)	Colony diameter (cm, d)	D/d
Penicillium viridicatum	3.51	1.49	2.36
Fusarium graminearum	2.70	1.08	2.50
Aspergillus flavus	3.15	1.06	2.97

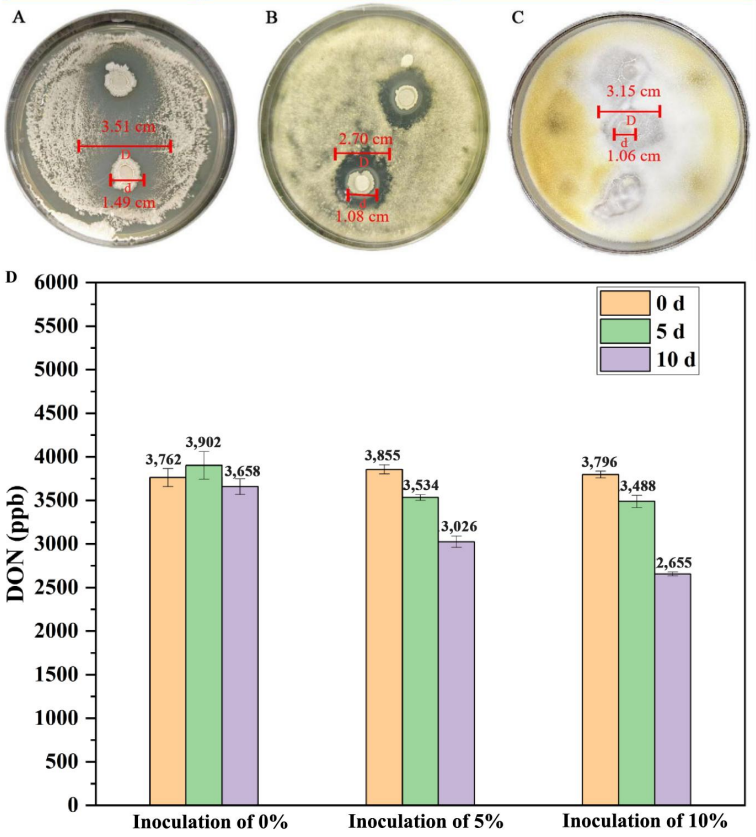

Figure. 6 Antifungal activity and DON removal capacity of *B. velezensis* T-3. (A) Plate confrontation assay against *P. viridicatum*; (B) Plate confrontation assay against *F. graminearum*; (C) Plate confrontation assay against *A. flavus*; (D) DON removal rates in moldy feed. **NOTE:** "D" denotes the inhibition zone diameter, while "d" denotes the fungal colony diameter. Copyright: This figure was created by the authors based on experimental data. The plate confrontation assay images (Figure. 6(A)−6(C)) are original photographs taken during the experiments. Representative images from three independent biological replicates are shown. The DON removal curve (Figure. 6(D)) was plotted using GraphPad Prism 8.0 based on ELISA-quantified data. Data are mean ± SD, n = 3 biological replicates. Error bars represent standard deviation.

4. Discussion

4.1. From Detoxification by Whole Cells to a Defined Enzyme Candidate

This study advances the interpretation of *B. velezensis* T-3 from a strain that detoxifies at the whole-cell level toward a more clearly defined system centered on the enzyme by identifying a *CotA*-type laccase candidate and linking it to a measurable DON-removal phenotype. Classical studies established *CotA* as a copper-dependent, highly stable laccase associated with the *Bacillus* spore coat[24,25]; however, recent reviews continue to note that many reports on mycotoxin detoxification mediated by *Bacillus* remain descriptive and fail to resolve the catalytic components responsible for toxin conversion. Against this backdrop, the identification of a *CotA* gene in a safe *B. velezensis* strain derived from sea cucumber gut is significant, as it provides a specific molecular target within a relevant probiotic background and extends research on mycotoxins associated with *CotA* beyond the more commonly studied *B. subtilis* and *B. licheniformis* systems[26].

While identification based on the genome provides a strong foundation for candidate enzyme discovery, the mere presence of a gene does not guarantee its active expression under relevant physiological conditions. In this study, we further employed 4D-DIA quantitative proteomics to directly validate the translation of the *CotA* gene in *B. velezensis* T-3. The detection of 23 unique and shared peptides, including a strictly proteotypic peptide (PLKEADTSRK), along with a cumulative intensity exceeding 376,000, provides strong evidence that confirms that *CotA* is not merely an artifact of the genome annotation but a genuinely expressed protein. This proteomic evidence bridges the gap between genotype and phenotype, substantially strengthening the link between the identified *CotA* gene and the observed activity of degrading DON. To our knowledge, this study represents one of the few reports that combine genome mining, structural modeling, and proteomic validation to characterize a laccase involved in mycotoxin removal in *B. velezensis*.

4.2. Structural Basis for DON Recognition

A central finding of this work is that the T-3 *CotA* possesses a plausible structural basis for DON recognition. The protein retains the

characteristic multicopper oxidase domains and conserved copper-binding residues of canonical *CotA*-like laccases, and docking analysis suggests that DON can be stabilized by THR260, THR262, GLY323, and THR418, with a binding energy of -6.299 kcal/mol and a distance of 6.40 Å from the T1 copper center. We emphasize that this docking model provides a computational hypothesis for DON recognition by *CotA*, rather than proof of catalytic turnover. This geometry is compatible with substrate accommodation and potential oxidation mediated by electron transfer. Nonetheless, the strength of this conclusion should be interpreted with appropriate caution. In the DON field, a higher standard has been established by studies such as that of Yang *et al*. who combined structural analysis, mutagenesis, and enzyme engineering to demonstrate that Arg68 is essential for Fhb7 activity and that engineered variants markedly improve DON detoxification performance[4]. Accordingly, the present data support a robust hypothesis rather than definitive proof of *CotA*-catalyzed DON turnover. Even so, this interpretation is well grounded in prior evidence showing that laccase systems can indeed transform DON. Hao *et al*. reported that Lac-W degraded DON by 34% within 24 h without redox mediators, whereas Jia *et al*., showed that mediator supplementation increased DON removal to 51% with ABTS and to 68% in a dual-mediator system with two mediators[5,6]. Shanakhat *et al*. further demonstrated DON modification by a system consisting of a fungal laccase and TEMPO[7]. Collectively, these studies support the biological plausibility that the *CotA* of *B. velezensis* T-3 participates in oxidative DON conversion.

The phenotypic results further suggest that the practical value of *B. velezensis* T-3 lies in its combined antifungal and detoxifying capacity under fermentation conditions. *B. velezensis* T-3 strongly inhibited *F. graminearum*, *A. flavus*, and *P. viridicatum*, and reduced DON by up to 30.06% after 10 days in the feed fermentation assay. Although this efficiency is lower than that reported for some optimized systems that use purified enzymes, the comparison should be interpreted in context. Cai *et al*. showed that *B. velezensis* T-3 derived from the gut of a sea cucumber completely eliminated the DON signal within 72 h in a liquid system where DON served as the sole carbon source[9], whereas the present work evaluated detoxification in a complex fermented feed matrix, where substrate heterogeneity, microbial competition, and limitations due to mass transfer are expected to constrain apparent efficiency. Likewise, Gao *et al*., obtained strong detoxification performance with recombinant *CotA* under conditions where mediators were used to assist in degrading AFB1 and ZEN[27]. Therefore, the more moderate DON reduction observed here does not weaken the significance of the study; rather, it indicates that a safe *B. velezensis* strain can function under a more practical substrate matrix while simultaneously limiting fungal proliferation and toxin burden.

DON is not a classical phenolic laccase substrate. Based on the docking geometry (6.4 Å from T1 copper, hydrogen bonds with THR260/THR262/GHR323/THR418), we propose that oxidation may occur at the C_9-C_{10} double bond or the C_3-OH group of the trichothecene core. This hypothesis requires experimental validation through site-directed mutagenesis and product identification.

4.3. Synergy Between Antifungal and Detoxifying Activities Shows Great Application Value

More broadly, the present findings support the view that *B. velezensis* is a promising chassis for discovering and engineering mycotoxin-detoxifying enzymes. The combined antifungal and detoxifying activities, together with the previously documented safety profile of this strain[9], highlight its potential for practical feed applications. Wei *et al*. showed that a *CotA*-like laccase from *B. velezensis B.*26 removed 91.94% of zearalenone within 6h under alkaline conditions and at high temperature[8], while Liu *et al*. demonstrated that rational engineering of *B. licheniformis CotA* markedly improved AFB1 degradation efficiency[28]. These studies highlight the feasibility of improving *CotA* performance through optimization guided by the protein structure and make the predicted residues that contact DON (identified here) attractive targets for future mutational validation. Overall, the main significance of this work lies in connecting a defined *CotA* candidate, a credible DON-binding model, and a phenotype that combines antifungal and detoxifying activities in whole cells within the same *B. velezensis* system. Future studies should therefore focus on heterologous expression of T-3 *CotA*, identification of DON transformation products, toxicity evaluation of those products, and site-directed validation of the predicted substrate-contact residues, which together will determine whether this enzyme can be developed as an independent biocatalyst or as part of a biodetoxification strategy that relies on the strain itself.

The complementary proteomic validation provided in this work addresses a critical limitation commonly seen in genome-mining studies, where candidate enzymes are proposed based solely on sequence homology. Here, we demonstrate that the *CotA* transcript is translated into a stable protein with high peptide coverage (47.30%) and substantial abundance, further corroborating its physiological relevance in DON binding and removal. Future studies should focus on heterologous expression of this *CotA* whose expression was validated by proteomics, followed by in vitro activity assays and product toxicity evaluation, to definitively establish its catalytic role in DON detoxification.

4.4. Limitations of This Study

We acknowledge that the present study has several limitations that should be considered when interpreting the findings. First, the DON reduction experiments were performed using whole-cell suspensions of *B. velezensis* T-3 rather than purified *CotA* protein. Consequently, we cannot definitively attribute the observed DON removal (30.06% in feed, 10 days) solely to *CotA* enzymatic activity, as other cellular components, metabolic pathways, or physical adsorption may have contributed to the overall reduction. Second, DON quantification was carried out by ELISA in a complex feed matrix; matrix effects and cross-reactivity cannot be completely excluded. Third, the molecular docking and structural modeling provide a computational hypothesis for DON recognition by *CotA*, but require experimental validation through site-directed mutagenesis and enzymatic assays. Despite these limitations, our integrative approach — combining genomic identification, proteomic expression validation, structural modeling, and phenotypic assays — provides a robust foundation for identifying *CotA* as a prime candidate for DON reduction in *B. velezensis* T-3. Future work will focus on heterologous expression of *CotA*, purification, and in vitro enzymatic characterization to definitively establish its catalytic role in DON detoxification.

5. Conclusion

In this study, we identified a *CotA* gene in the safe *B. velezensis* T-3 isolated from sea cucumber gut. The encoded *CotA*

protein exhibits a typical multicopper oxidase structure, extracellular localization, and a favorable binding mode with DON. Molecular docking simulations demonstrated stable binding of DON to *CotA* via hydrogen bonds, with a distance of 6.4 Å from the T1 copper center, suggesting catalytic potential. Importantly, 4D-DIA quantitative proteomic analysis provided supportive evidence that *CotA* is actively expressed in T-3 under standard culture conditions, with high peptide coverage (47.30%) and substantial abundance (cumulative intensity > 376,000). This proteomic validation substantiates that the *CotA* gene is not merely an annotation from the genome but a genuine functional protein, thereby strengthening the link between the genotype and the observed phenotype of degrading DON. Experimental results further showed that *B. velezensis* T-3 could inhibit the growth of toxigenic fungi and significantly reduce DON content in feed, achieving a 30.06% removal rate within 10 days. This work provides a candidate strain and a theoretical foundation for the development of novel feed detoxification agents. Nevertheless, the enzymatic activity of purified *CotA* toward DON remains to be experimentally verified in future studies, and the transformation products and their toxicological profiles require further investigation.

Author Contributions

Xinghua Cai and Jiali Su: conceptualization, funding acquisition, review and editing. Xinghua Cai, Jiali Su, and Yanhong Cao: methodology, investigation, and writing – original draft. Ngo Dinh Tan, Miao Liang, Qianyi Chen, and Shasha Luo: data curation, formal analysis. Jiali Su, Fengdie Huang, Xinghua Cai, and Dong Luo: methodology, software. Xinghua Cai, Yanhong Cao, and Ngo Dinh Tan: validation, visualization. all authors read and approved the final manuscript.

Artificial Intelligence (AI) Statements

No artificial intelligence (AI) tools were used in the preparation of this manuscript.

Conflicts of Interest

The authors declare they have no competing interests.

Supplementary Information

The **supplementary** data of this article can be found at the online version.

Data Availability

The metagenomic sequencing data generated in this study have been deposited in the National Center for Biotechnology Information (NCBI) under the accession number of PRJNA1417926 (https://www.ncbi.nlm.nih.gov/bioproject/PRJNA1417926). The raw mass spectrometry proteomics data have been provided as Supplementary File accompanying this submission.

Funding

This research was supported by the Guangxi Science and Technology Project (Gui Ke Nong AB2506910017), National Key R&D Program of China (2022YFD1300602), Natural Science Foundation of Guangxi of China (2024GXNSFDA010039), the Innovation Project of Guangxi Graduate Education (Grant No. YCBZ2023050).

References

[1] Lin Y, Wang R, Liu S, *et al.* Deoxynivalenol and Its Metabolites: Contamination, Metabolism, and Toxicity. *Toxins* (*Basel*). 2025, 17 (11): 1-20. [Google Scholar] [CrossRef]

[2] Moreno J, Nielsen H, Winther O, *et al.* Predicting the subcellular location of prokaryotic proteins with DeepLocPro. *Bioinformatics*. 2024, 40 (12): 1-5. [Google Scholar] [CrossRef]

[3] Enguita FJ, Leitão AL. Cross-Kingdom Enzymatic Strategies for Deoxynivalenol Detoxification: Computational Analysis of Structural Mechanisms and Evolutionary Adaptations. *Microorganisms*. 2025, 13 (10): 1-24. [Google Scholar] [CrossRef]

[4] Yang J, Liang K, Ke H, *et al.* Enzymatic Degradation of Deoxynivalenol with the Engineered Detoxification Enzyme Fhb7. *JACS Au*. 2024, 4 (2): 619-634. [Google Scholar] [CrossRef]

[5] Hao WB, Gu X, Yu X, *et al.* Laccase Lac-W detoxifies aflatoxin B1 and degrades five other major mycotoxins in the absence of redox mediators. *Environmental Pollution*. 2023, 338: 1-10. [Google Scholar] [CrossRef]

[6] Jia M, Yu X, Xu K, *et al.* The High-Efficiency Degradation of Multiple Mycotoxins by Lac-W Laccase in the Presence of Mediators. *Toxins (Basel)*. 2024, 16 (11): 1-13. [Google Scholar] [CrossRef]

[7] Shanakhat H, McCormick SP, Busman M, *et al.* Modification of Deoxynivalenol by a Fungal Laccase Paired with Redox Mediator TEMPO. *Toxins (Basel)*. 2022, 14 (8): 1-16. [Google Scholar] [CrossRef]

[8] Wei Z, Zhang X, Shi L, *et al.* Functional Characterization and Mechanism of Two Zearalenone-Degrading Enzymes from *Bacillus velezensis* B.26. *Journal of Agricultural and Food Chemistry*. 2025, 73 (23): 14629-14640. [Google Scholar] [CrossRef]

[9] Cai X, Luo S, Chen X, *et al.* Whole genome sequencing and metabonomics analysis reveal the biodegradation process of deoxynivalenol in a safety *Bacillus velezensis* T-3 isolated from the gut of sea cucumber. *Food Chemistry: X*. 2025, 31: 1-13. [Google Scholar] [CrossRef]

[10] Teufel F, Almagro Armenteros JJ, Johansen AR, *et al.* SignalP 6.0 predicts all five types of signal peptides using protein language models. *Nature Biotechnology*. 2022, 40 (7): 1023-1025. [Google Scholar] [CrossRef]

[11] Hallgren J, Tsirigos K D, Pedersen M D, *et al.* DeepTMHMM predicts alpha and beta transmembrane proteins using deep neural networks. *bioRxiv*. 2022: 1-12. [Google Scholar] [CrossRef]

[12] Gasteiger E, Hoogland C, Gattiker A, *et al.* Protein Identification and Analysis Tools on the ExPASy Server. In: Walker JM, ed. *The Proteomics Protocols Handbook*. Humana Press; 2005: 571-607. [Google Scholar] [CrossRef]

[13] Jones P, Binns D, Chang HY, *et al.* InterProScan 5: genome-scale protein function classification. *Bioinformatics*. 2014, 30 (9): 1236-1240. [Google Scholar] [CrossRef]

[14] Demichev V, Messner CB, Vernardis SI, *et al.* DIA-NN: neural networks and interference correction enable deep proteome coverage in high throughput. *Nature Methods*. 2020, 17 (1): 41-44. [Google Scholar] [CrossRef]

[15] Kumar S, Stecher G, Tamura K. MEGA7: Molecular Evolutionary Genetics Analysis Version 7.0 for Bigger Datasets. *Molecular Biology and Evolution*. 2016, 33 (7): 1870-1874. [Google Scholar] [CrossRef]

[16] Larkin MA, Blackshields G, Brown NP, *et al*. Clustal W and Clustal X version 2.0. *Bioinformatics*. 2007, 23 (21): 2947-2948. [Google Scholar] [CrossRef]

[17] Gouet P, Robert X, Courcelle E. ESPript/ENDscript: Extracting and rendering sequence and 3D information from atomic structures of proteins. *Nucleic Acids Research*. 2003, 31 (13): 3320-3323. [Google Scholar] [CrossRef]

[18] Abramson J, Adler J, Dunger J, *et al*. Accurate structure prediction of biomolecular interactions with AlphaFold 3. *Nature*. 2024, 630 (8016): 493-500. [Google Scholar] [CrossRef]

[19] Pettersen EF, Goddard TD, Huang CC, *et al*. UCSF Chimera--a visualization system for exploratory research and analysis. *Journal of Computational Chemistry*. 2004, 25 (13): 1605-1612. [Google Scholar] [CrossRef]

[20] Kim S, Chen J, Cheng T, *et al*. PubChem 2025 update. *Nucleic Acids Research*. 2025, 53 (D1): D1516-D1525. [Google Scholar] [CrossRef]

[21] Seeliger D, de Groot BL. Ligand docking and binding site analysis with PyMOL and Autodock/Vina. *Journal of Computer-Aided Molecular Design*. 2010, 24 (5): 417-422. [Google Scholar] [CrossRef]

[22] Bugnon M, Röhrig UF, Goullieux M, *et al*. SwissDock 2024: major enhancements for small-molecule docking with Attracting Cavities and AutoDock Vina. *Nucleic Acids Research*. 2024, 52 (W1): W324-W332. [Google Scholar] [CrossRef]

[23] Trott O, Olson AJ. AutoDock Vina: improving the speed and accuracy of docking with a new scoring function, efficient optimization, and multithreading. *Journal of Computational Chemistry*. 2010, 31 (2): 455-461. [Google Scholar] [CrossRef]

[24] Jones SM, Solomon EI. Electron transfer and reaction mechanism of laccases. *Cell Mol Life Cellular and Molecular Life Sciences*. 2015, 72 (5): 869-883. [Google Scholar] [CrossRef]

[25] Martins LO, Soares CM, Pereira MM, *et al*. Molecular and biochemical characterization of a highly stable bacterial laccase that occurs as a structural component of the *Bacillus subtilis* endospore coat. *Journal of Biological Chemistry*. 2002, 277 (21): 18849-18859. [Google Scholar] [CrossRef]

[26] Nguyen T, Chen X, Ma L, *et al*. Mycotoxin Biodegradation by *Bacillus* Bacteria-A Review. *Toxins (Basel)*. 2024, 16 (11): 1-24. [Google Scholar] [CrossRef]

[27] Gao B, An W, Wu J, *et al*. Simultaneous Degradation of AFB1 and ZEN by *CotA* Laccase from *Bacillus subtilis* ZJ-2019-1 in the Mediator-Assisted or Immobilization System. *Toxins (Basel)*. 2024, 16 (10): 1-16. [Google Scholar] [CrossRef]

[28] Liu Y, Liu L, Huang Z, *et al*. Combined Strategies for Improving Aflatoxin B1 Degradation Ability and Yield of a *Bacillus licheniformis CotA*-Laccase. *International Journal of Molecular Sciences*. 2024, 25 (12): 1-11. [Google Scholar] [CrossRef]